


# Measuring the anisotropic conductivity of rub-aligned doped semiconducting polymer films: The role of electrode geometry

Quynh M. Duong,<sup>1,†</sup> Diego Garcia Vidales,<sup>1,†</sup> Charlene Z. Salamat,<sup>1</sup> Sarah H. Tolbert,<sup>1,2</sup> and Benjamin J. Schwartz<sup>1,\*</sup>

<sup>1</sup>*Department of Chemistry and Biochemistry, University of California Los Angeles, Los Angeles, California 90095-1569, United States*

<sup>2</sup>*Department of Materials Science and Engineering, University of California Los Angeles, Los Angeles, California, 90095-1595, United States*

 (Received 3 July 2023; revised 21 November 2023; accepted 2 January 2024; published 2 February 2024)

Doped semiconducting polymers are attractive for optoelectronic applications due to their solution processibility, low cost, flexibility, and potential for use in near-room-temperature thermoelectric generators. One way to improve charge transport in doped conjugated polymer films is to orient all the polymer chains in the same direction via rub-aligning, although aligned doped polymer films have an anisotropic electrical conductivity. Here, we compare the use of different electrode geometries to measure the anisotropic conductivity of rub-aligned doped poly(3-hexylthiophene-2,5-diyl) (P3HT) films. We show that for P3HT films doped both conventionally with 2,3,5,6-tetrafluoro-7,7,8,8-tetracyanoquinodimethane (F<sub>4</sub>TCNQ) and via anion exchange with F<sub>4</sub>TCNQ and lithium bis(trifluoromethanesulfonyl)imide, a rectangular electrode geometry in combination with the modified Montgomery method can determine the anisotropic conductivity as accurately as the use of the Hall bar geometry. This rectangular geometry provides two significant advantages. First, the rectangular electrode geometry is much simpler to fabricate than the standard Hall bar geometry. Second, the rectangular geometry requires only a single sample to obtain both components of the anisotropic conductivity, unlike the Hall bar geometry for which two separate samples are required. This is particularly important for rub-aligned doped conjugated polymer films, which have large sample-to-sample variabilities. We also explore anisotropic Hall effect measurements of rub-aligned doped polymer films, and examine the use of a four-line electrode geometry, which has been popular in the literature for measuring the anisotropic conductivities of rub-aligned doped conjugated polymer films. We find that the four-line geometry overestimates the conductivity by approximately 40%.

DOI: [10.1103/PhysRevApplied.21.024006](https://doi.org/10.1103/PhysRevApplied.21.024006)

## I. INTRODUCTION

With their intrinsically low thermal conductivities, semiconducting conjugated polymers such as poly(3-hexylthiophene-2,5-diyl) (P3HT) are materials with promising potential for thermoelectric applications [1–3]. However, pristine semiconducting polymers also possess poor electrical conductivity,  $\sigma$ , which affects the thermoelectric efficiency  $zT$ ,

$$zT = \frac{S^2 \sigma}{\kappa} T, \quad (1)$$

where  $S$  is the Seebeck coefficient,  $\sigma$  is the electrical conductivity,  $\kappa$  is the thermal conductivity, and  $T$  is the temperature. The electrical conductivity of

semiconducting polymer films is in turn determined by carrier density  $n$  and mobility  $\mu$ :  $\sigma = ne\mu$ , where  $e$  is the fundamental charge.

The carrier density in semiconducting polymers can be increased by doping; most conjugated polymers are  $p$ -type materials and thus can be doped with strong oxidizing agents, such as 2,3,5,6-tetrafluoro-7,7,8,8-tetracyanoquinodimethane (F<sub>4</sub>TCNQ). The carrier mobility, however, is heavily dependent on a doped polymer film's morphology. In general, most conjugated polymers are semicrystalline, which means that outside of the relatively small crystallites, the chains in conjugated polymer films can bend, twist, and entangle, resulting in randomly oriented ordered and amorphous regions. This bending and twisting can break the conjugation, leading to a broad distribution of conjugated sites with different energies [4]. Charge transport in the presence of such site disorder is generally poor and mainly dictated by thermally activated hopping [4–6].

\*schwartz@chem.ucla.edu

†These authors contributed equally to this work

One route to reduce energetic disorder and thus improve carrier mobility is to molecularly align the chains in doped conjugated polymer films. A versatile way to achieve this is via high-temperature rubbing, a method pioneered by Brinkmann and coworkers, which macroscopically aligns the polymer chains along the rubbing direction [7–14]. The rubbing process significantly enhances the electrical conductivity compared to non-aligned films, with reports of the conductivity of F<sub>4</sub>TCNQ-doped P3HT films increasing from 9 to 160 S/cm after rub alignment [7].

Although the electrical conductivity of rub-aligned doped conjugated polymer films is significantly enhanced compared to that of nonaligned films, the charge transport in such films is anisotropic [7,15–17]. This is because carrier transport mainly occurs along the conjugated backbone and between chains that are  $\pi$ -stacked; transport is not facile through the electrically insulative side chains that confer solubility [18]. Thus, anisotropic electrical conductivity measurements are often reported in terms of conductivities parallel ( $\parallel$ ) and perpendicular ( $\perp$ ) to the rubbing direction [7–14,19], and these values can differ by a factor of 3.5 to 8 [7,9]. Here, our goal is to explore the merits of different methods for measuring anisotropic electrical conductivities in rub-aligned doped conjugated polymer films.

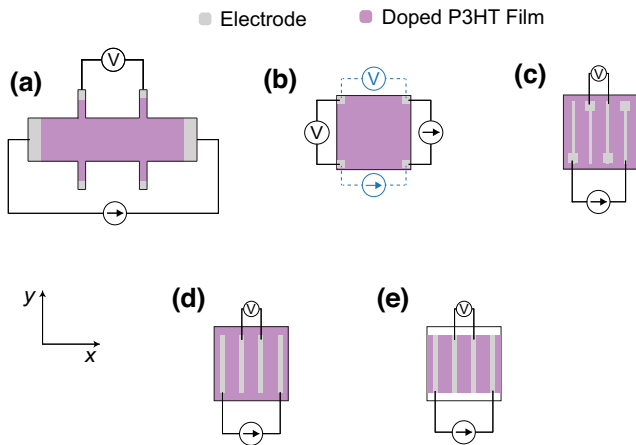


FIG. 1. Geometries of the different methods for anisotropic conductivity measurements on doped rub-aligned conjugated polymers explored in this work: (a) the standard six-contact Hall bar geometry; (b) the rectangular geometry via the Montgomery method, where the source current and voltage measurements are rotated by 90° (denoted by blue and black) along the principal  $x$  and  $y$  axes; (c) the four-line geometry similar to that used by Brinkmann and coworkers [7,9–14]; (d) the rectangular four-line geometry; and (e) the rectangular four-line confined geometry. Here, the purple shading represents the aligned doped P3HT film, the gray shading shows the positions of the electrodes, the arrow indicates a current source, and V indicates a voltage measurement.

The standard way to obtain anisotropic conductivities and/or resistivities is using a four-point probe measurement with electrodes arranged in the Hall bar geometry, which is shown in Fig. 1(a). The source and sink electrodes are placed on opposite ends of a rectangular strip, confining current flow to a single direction. However, fabricating a Hall bar electrode geometry is often not simple or convenient, and only one conductivity direction can be measured per sample. This is particularly problematic for rub-aligned conjugated polymer films, for which there is a great deal of sample-to-sample variation as well as variances between different locations on the same sample, so that it can be challenging to compare conductivities in different directions taken on different samples or even in different places on the same film.

Here, we show that the anisotropic conductivity of rub-aligned films can be measured accurately using a simpler rectangular geometry [Fig. 1(b)] based on the revised Montgomery method [20,21], which also provides the advantage that the parallel and perpendicular conductivities of rub-aligned films can be measured on the same sample and location. We also explore the possibility of performing Hall effect measurements on rub-aligned films using this rectangular geometry and we show that four-line [Fig. 1(c)] measurements used by Brinkmann and coworkers for anisotropically conducting doped conjugated polymer samples significantly overestimate the conductivity.

## II. RESULTS AND DISCUSSION

The Montgomery method [22] is a technique that combines the work of Wasscher [23], van der Pauw [24], and Logan *et al.* [25] to deconvolute the different directional resistivities in anisotropic materials. Unlike the Hall bar geometry, the samples used in the Montgomery method are fabricated into a simple rectangular geometry, as shown in Fig. 1(b), with electrodes placed at each corner. The method requires that the direction of the components of the resistivity ( $\rho_i$ ) be along the sample's principal axes,  $i = x$  or  $y$ . Since the directions of the resistivity components are known in rub-aligned films through polarized UV-visible (UV-vis) spectroscopy, only two resistance measurements are needed to solve for the film's anisotropic conductivity.

Figure 2 illustrates the relationship between the anisotropic sample and its isotropic equivalent. Both  $L'_i$  and  $L_i$  have units of length, with the prime referring to the anisotropic samples and the nonprimed variables referring to the isotropic equivalent. Through the Wasscher transformation, the anisotropic problem is now an isotropic one with a single resistivity  $\rho$ ,

$$\rho = H_x E R_x = H_y E R_y, \quad (2)$$

where the isotropic resistivity is based on the resistances ( $R_i$ ) measured in the in-plane principal directions with two

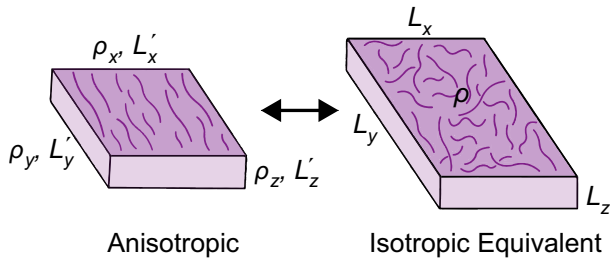


FIG. 2. Schematic of the Wasscher transformation of anisotropically conducting samples with conductivity  $\rho_i$  along the principal axes with lengths  $L'_i$  into an isotropically conducting equivalent with lengths  $L_i$ . The key step of the Montgomery method is mapping the anisotropically conducting sample onto that of an isotropic equivalent using the Wasscher transformation, which treats the anisotropic sample as isotropic but with dimensions proportional to its anisotropic resistivity [23].

correction factors,  $H_i$  and  $E$ . The correction factors  $H_i$  account for the finite lateral dimensions, while  $E$  accounts for the finite thickness of the isotropic sample [20,21]. Logan *et al.* solved the above relation using the method of images and obtained a series for the correction factors [25].

A revision of the Montgomery method by dos Santos *et al.* [20] simplified the series by showing that only the first term was needed to obtain a good approximation. For this revised version, the  $H_i$ 's are simplified to

$$H_x \approx \left(\frac{\pi}{8}\right) \sinh\left(\frac{\pi L_y}{L_x}\right) \quad \text{and} \quad H_y \approx \left(\frac{\pi}{8}\right) \sinh\left(\frac{\pi L_x}{L_y}\right). \quad (3)$$

The  $H_i$  correction factors in Eq. (3) depend only on the ratio between the isotropic in-plane dimensions  $L_x$  and  $L_y$ . The value of this ratio is proportional to the resistance ratio measured in the two principal directions. Using the definition  $\sinh(x) = (e^x - e^{-x})/2$  and Eqs. (2) and (3), dos Santos *et al.* [20] obtained the following approximation that can be used to calculate the  $H_i$ 's:

$$\frac{L_y}{L_x} \cong \frac{1}{2} \left[ \frac{1}{\pi} \ln \frac{R_y}{R_x} + \sqrt{\left(\frac{1}{\pi} \ln \frac{R_y}{R_x}\right)^2 + 4} \right]. \quad (4)$$

With the help of Eq. (4), the correction factors  $H_i$  can be easily obtained through two resistance measurements along the principal axes, allowing the anisotropic resistivity components to be straightforwardly determined by reversing the Wasscher transformation, as summarized in Eq. (5) [20,21],

$$\begin{aligned} \rho_x &\approx \left(\frac{\pi}{8}\right) E' \left(\frac{L'_y}{L_x}\right) \left(\frac{L_x}{L_y}\right) R_y \sinh\left[\frac{\pi L_x}{L_y}\right] = \frac{1}{\sigma_x} \\ \text{and} & \\ \rho_y &\approx \left(\frac{\pi}{8}\right) E' \left(\frac{L'_x}{L_y}\right) \left(\frac{L_y}{L_x}\right) R_x \sinh\left[\frac{\pi L_x}{L_y}\right] = \frac{1}{\sigma_y}. \end{aligned} \quad (5)$$

For thin-film samples, the effective anisotropic thickness  $E'$  can be replaced with the actual sample thickness  $L'_z$ . With the revised Montgomery method, the anisotropic conductivities can thus be obtained with two simple resistance measurements without having to fabricate multiple rub-aligned samples. Furthermore, Eq. (5) also gives us a generic relation between the anisotropic resistivity components and the anisotropic conductivity ( $\sigma_x$  and  $\sigma_y$ ).

To test how well this formalism works on doped aligned films of semiconducting polymers, we employed the high-temperature rub-aligning method to create anisotropic P3HT films [7–9]. The polymer films were made by spin coating regioregular (97%) P3HT (Ossila) onto glass substrates. After allowing them to dry, the P3HT films were then rub-aligned at 140 °C using a homemade setup consisting of a microfiber polishing wheel that can be applied to the film with a reproducible force in an inert atmosphere (see Fig. S1 and other details in the Supplemental Material [26–29]). Polarized UV-vis spectroscopy (Fig. S2 in the Supplemental Material [26]) showed that the dichroic ratio ( $I_{\parallel}/I_{\perp}$ ) of the absorbance at 610 nm (2.03 eV) was  $\geq 10$ , comparable to the highest dichroic ratios previously reported for rub-aligned P3HT [7–14,19]. We also saw a small enhancement of the 0-0 vibrational peak relative to the 0-1, which is indicative of the stronger intrachain coupling that results from straightening the polymer chains [7,30–32].

After successfully rub-aligning the P3HT films, we then chemically doped them using the sequential processing method, which involves exposing the samples to a solution of the dopant in a solvent that swells but does not dissolve the underlying polymer film [31,33–35]. One set of aligned P3HT samples was doped with a solution of 3-mg/ml  $F_4TCNQ$  (Ossila) in *n*-butyl acetate (*n*-BA). The second set of samples was doped using the anion-exchange method [36] by exposing the films to a solution of 3-mg/ml  $F_4TCNQ$  in *n*-BA that was codissolved with 30 mg/ml of bis(trifluoromethane)sulfonimide lithium (LiTFSI) electrolyte. The anion-exchange method allows for higher doping levels than conventional doping methods and provides control over the counterion present in the rub-aligned doped polymer film [19].

Figure 3 shows polarized UV-vis absorption spectra for the rub-aligned P3HT films doped with each of these two methods. For the conventional doping method, Fig. 3(a) shows that light polarized  $\parallel$  to the rubbing direction probes the neutral P3HT band-gap absorption near 2.2 eV as well as the so-called  $P2$  (around 1.6 eV) and  $P1$  ( $< 1$  eV) peaks associated with the presence of polarons (charge carriers). With light polarized in the  $\perp$  direction, we see that the neutral polymer absorption is significantly blue-shifted to around 2.4 eV, and we also see  $F_4TCNQ$  anion peaks at around 1.4, 1.6, and 3.0 eV. The small presence of these anion peaks seen in the parallel direction indicates that not

all of the doped polymer chains are fully aligned in the rubbing direction.

In contrast to the conventional doping method, the polarized absorption spectra of the anion-exchange-doped films shown in Fig. 3(b) no longer show the presence of the F<sub>4</sub>TCNQ anion, indicating that the F<sub>4</sub>TCNQ anions were successfully exchanged with TFSI anions [19,36]. We also observe the presence of the P1 and P2 polaron absorption features in the perpendicular direction, indicating that the extra doping power afforded by the anion-exchange method allows for doping some of the amorphous regions that remain in the aligned film. This idea is also supported by a decrease in the intensity of the blue-shifted P3HT band-gap peak in the perpendicular direction: with anion exchange, there are fewer undoped and more doped conjugated segments that are not aligned along the rubbing direction [19]. Thus, our use of conventional and anion-exchange doping allows us to get better insights into how having carriers in different regions (aligned and crystalline in the conventionally doped films versus crystalline and amorphous in the anion-exchange-doped films) affects the anisotropic electrical conductivity.

For our electrical measurements on the rub-aligned, doped P3HT films, we limited the source current to 10  $\mu$ A to avoid injecting excess charges and to minimize sample heating, even though we found that for all of our samples in both the Hall bar and rectangular geometries, the current could be sourced up to 1 mA without any evidence of non-Ohmic behavior. We also note the rub-aligned P3HT films are quite rough [10,11], so that it is not straightforward to determine the thickness of these films. (The Brinkmann group suggested melting the films,

which destroys their alignment, and then using UV-vis spectroscopy to determine the average thickness postmelt [7–13].)

The primary and most commonly employed method for assessing the morphology and thickness of a thin film is either via profilometry or atomic force microscopy. Fig. S5 (see Supplemental Material [26]) displays three-dimensional (3D) surface profiles of nonaligned and rub-aligned P3HT films, both doped and undoped, obtained using profilometry. We note that the rub-aligning process significantly increases the surface roughness of the films, as imperfections on the surface of the microfiber polishing wheel cut grooves and ridges into the relatively soft polymer underneath. This increased roughness makes it difficult to accurately measure the rub-aligned thickness by the traditional method of making a cut into the film to expose the substrate and performing a line scan to determine the film thickness as the height of the step adjacent to the cut.

Thus, for our rub-aligned samples, instead of relying on a few individual line scans that can show large variations, we elected to determine the average thickness over a large area of each sample, as documented in Table S5 of the Supplemental Material [26]. We found that despite the rough topology, the average thickness and surface roughness of our rub-aligned films were reproducible, giving us confidence when comparing sheet resistances or conductivities between samples or measurements with different electrode geometries.

One feature worth noting is that the average profilometry-determined thickness of our rub-aligned films looks as if it is greater than the thickness of the nonaligned films

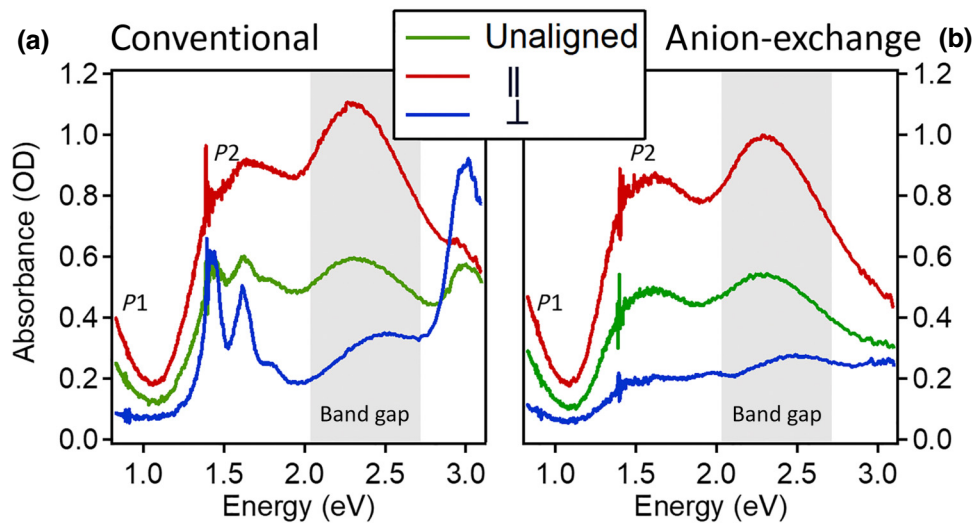


FIG. 3. Polarized UV-vis absorption spectra [red curves, light polarized parallel ( $\parallel$ ) to the rubbing direction; blue curves, light polarized perpendicular ( $\perp$ ) to the rubbing direction] of rub-aligned doped P3HT films; the green curves show the corresponding spectrum of an unaligned doped P3HT film. (a) Results for conventional doping with F<sub>4</sub>TCNQ; (b) results for doping via the anion-exchange method in the presence of LiTFSI. The noise near 1.4 eV is due to a lamp change in the instrument. OD, optical density.

TABLE I. Conductivity of nonaligned and rub-aligned doped P3HT films measured using both the Hall bar [Fig. 1(a)] and rectangular [Fig. 1(b)] electrode geometries.

Conductivity (S/cm)	Rectangular nonaligned	Hall bar nonaligned	Rectangular aligned ( $\parallel$ , $\perp$ )	Hall bar aligned ( $\parallel$ , $\perp$ )
Conventionally-doped	$4.66 \pm 0.30$	$4.25 \pm 1.18$	$8.28 \pm 0.12$ , $0.63 \pm 0.09$	$9.89 \pm 2.81$ , $0.91 \pm 0.31$
Anion-exchange-doped	$12.36 \pm 0.19$	$11.07 \pm 0.36$	$33.95 \pm 0.09$ , $3.22 \pm 0.36$	$47.43 \pm 23.3$ , $3.41 \pm 0.66$

from which they were prepared. This appears counterintuitive, as the rubbing process is expected to remove polymer material, so that the rub-aligned films would be expected to become thinner. However, the roughness features on the surface of the film are comparable to or smaller in size than the profilometer tip diameter, which is thus unable to properly measure the depth of the grooves rubbed into the films' surfaces. The conductivities we report in Table I use the average thickness determined by the 3D profilometry scans are thus likely underestimated since the thickness we use to calculate the conductivities is likely overestimated, as discussed in more detail in the Supplemental Material [26]. This slight systematic error, however, does not affect our comparison of the use of different electrode geometries to measure the anisotropic conductivity of our rub-aligned samples.

Table I summarizes the electrical conductivity measurements for our conventionally and anion-exchange-doped nonaligned and rub-aligned P3HT films. The reported values were averaged from at least three independent samples. The conductivities measured via the rectangular geometry are the same within error as those measured using the Hall bar geometry, verifying that the rectangular method can accurately measure the anisotropic conductivity of aligned doped conjugated polymer films. The modest discrepancies between the conductivities obtained using the two methods are largely due to sample-to-sample variations, as it is quite challenging to make precisely identical rub-aligned films, and the measurements made with different electrode geometries must be taken on different samples. Fortunately, the rectangular geometry allows both the parallel and perpendicular measurements to be taken simultaneously on the same sample, a significant advantage over the Hall bar geometry.

The parallel and perpendicular conductivities of the rub-aligned P3HT films doped with the conventional method are  $8.28 \pm 0.12$  and  $0.63 \pm 0.09$  S/cm (averaged values from the modified Montgomery method), respectively. As has been discussed previously [7–9], the doped rub-aligned films show a higher parallel conductivity compared with doped nonaligned films ( $4.66 \pm 0.30$  S/cm), the result of improved charge transport in the rub-aligned direction. The conductivity of the rub-aligned doped films in the perpendicular direction, however, is significantly lower than

that of the nonaligned film. In addition to the fact that carrier transport in the  $\perp$  direction largely involves hopping between polymer chains, the decreased perpendicular conductivity may also result from the fact that rub-alignment induces a change in the texturing of the polymer [37].

Charge transport within doped semiconducting polymers is anisotropic on a molecular scale, since it is easier for carriers to move along the conjugated backbone of the polymer or between  $\pi$ -stacked chains than along the direction of the insulating side groups [18,38–41]. When spin-cast into thin films, P3HT crystallites tend to be edge-on oriented with respect to the substrate, so that the best molecular directions for electrical conductivity both lie in plane. However, rub-alignment of P3HT films results in the formation of both edge-on and face-on oriented crystallites [7–14,37], as shown in Fig. S3 of the Supplemental Material [26]. Thus, even though highly oriented polymer chains should have enhanced charge transport due to reduced energetic disorder, the fact that some crystallites now have their insulating side chains lying in plane may hinder the mobility of carriers on the molecular scale. This diminished conduction in the perpendicular direction has also been observed in a recent report involving rub-aligned doped conjugated polymer films utilizing the Hall bar geometry [19]. Numerous studies in the field of organic solar cells have also indicated that charge transport through the side chains is considerably less effective than traversing the  $\pi$  stacks or following the polymer backbone [42–45].

It is worth noting that our finding that the perpendicular conductivity of the rub-aligned doped P3HT film is lower than that of an isotropic film, which we believe makes sense, is in contrast to results presented by Untilova *et al.* [7]. These workers reported conductivity values for aligned doped conjugated polymers in the perpendicular direction that equaled or exceeded the conductivity of the corresponding nonaligned polymer samples. As we will discuss in more detail below, we believe that this result is an artifact of the fact that this group used a four-line electrode geometry, shown in Fig. 1(c) [7], which is not appropriate for determining the conductivity of anisotropically conducting samples.

For the rub-aligned P3HT films doped with the anion-exchange method, the parallel and perpendicular conductivities are much higher than those doped with the

conventional methods,  $33.95 \pm 0.09$  and  $3.22 \pm 0.36$  S/cm, respectively. The higher conductivities make sense given that the anion-exchange method leads to higher doping levels, which is consistent with the more depleted neutral P3HT band-gap absorption seen in Fig. 3(b). It is worth noting that even though anion exchange dopes the amorphous regions as well as the crystalline regions of the P3HT film, the anisotropy in the observed conductivities is actually slightly higher than that of the conventionally doped films. This suggests that electrical conduction through the amorphous regions is not substantial, even when the films are highly doped [46].

In addition to conductivity measurements, we also performed Hall effect measurements on the rub-aligned doped P3HT films in an effort to obtain insights into anisotropic carrier mobility. Typically, the Hall bar geometry is used to determine anisotropic carrier mobilities [47]. In contrast, the rectangular geometry based on the van der Pauw method is not commonly used for anisotropic samples because the results can be difficult to interpret due to the apparent dependence of the Hall voltage on the sample's anisotropy. However, Bierwagen *et al.* [47] have presented numerical calculations and experimental data showing that a sample's anisotropy does not have a significant impact on the measurement of the Hall voltage, so that it should be possible to utilize the van der Pauw geometry to calculate an anisotropic sample's carrier density and mobility without the need for a correction factor. Here, we used the revised Montgomery method, along with rectangular-geometry Hall measurements, to obtain the anisotropic sheet carrier density and thus the anisotropic mobility of the carriers in doped rub-aligned P3HT films, the results for which are summarized in Table II.

In principle, the carrier density should be the same regardless of the measured direction; this is because the same doping-induced charge carriers move either along or against the rubbing direction. However, with the Hall bar geometry, the carrier density measured in the parallel direction is roughly an order of magnitude less than that in the perpendicular direction. We believe that this is an effect of having mixed transport in the rub-aligned system. Only bandlike carrier transport is directly affected by the Lorentz force, so the presence of low-mobility carriers that move by hopping in doped organic semiconductors presents challenges for interpreting the results of Hall effect measurements [6,48,49]. Yi *et al.* have proposed a set of analytical expressions to describe Hall measurements in a simple isotropic system with two types of carrier transport: bandlike and hopping transport [6]. When a significant fraction of the carriers have hopping-like transport, the measured Hall carrier density can deviate significantly from the actual total carrier density.

We believe that the difference in Hall mobility and Hall carrier density observed in rub-aligned doped P3HT films is due to underestimating and overestimating the

total carrier density in the directions parallel and perpendicular to the rub alignment, respectively. For the Hall bar geometry in the parallel direction, we expect that more carriers would experience bandlike transport owing to the chain alignment. This is supported by temperature-dependent conductivity measurements on the rub-aligned films, which are presented in Figs. S6, S7, and Table S7 in the Supplemental Material [26]. The activation barrier for conduction extracted from these measurements is lower in the direction parallel to the rub-alignment than in the perpendicular direction; the parallel conduction barrier is also lower than that seen in the nonaligned doped films. The lower activation barrier is consistent with reduced energetic disorder, more delocalized carriers and thus a greater degree of bandlike versus hopping-like transport [50].

The small number of carriers that experience hopping-like transport will contribute little to the Hall voltage, so the measured Hall carrier density is slightly less than the total carrier density. In the perpendicular direction, however, carrier transport is primarily via hopping due to the need for interchain carrier motion, particularly due to the face-on polymer texture. Although hopping carriers are not affected directly by the Lorentz force, they are affected by the electric field caused by the separation of the transport of the small number of bandlike carriers [6]. This electric field forces the hopping carriers to move against the Lorentz force, resulting in a smaller measured Hall voltage and thus an overestimate of the carrier density.

Interestingly, the Hall carrier density determined using the rectangular geometry is closer to that measured via the Hall bar geometry in the perpendicular direction than the parallel direction. Since the current in the rectangular geometry is sourced about  $45^\circ$  to the parallel direction, the Hall voltage measured in this geometry should be a weighted average of the two transport cases mentioned above, with hopping transport more likely than bandlike transport. However, it is difficult to pinpoint which geometry gives the most correct measurement of the total carrier concentration without knowing the precise extent of the mixed transport effect. Clearly, electrode placement relative to the rubbing direction is crucial since it will govern the contribution of bandlike and hopping transport to the anisotropic Hall measurement.

Since they are much more highly doped, the anion-exchanged-doped aligned P3HT films are expected to have a higher carrier mobility due to a lower barrier for hopping [50]. Indeed, higher mobility was observed in both the aligned and nonaligned anion-exchange-doped samples than in those that were conventionally doped. However, we observed the same mobility anisotropy trend in the anion-exchange-doped samples, with higher mobility in the parallel direction obtained from the Hall bar geometry than that obtained from the rectangular geometry. Similar to the conventional doping case, this was due to a

TABLE II. dc-field and current-reversed Hall effect measurements for conventional and anion-exchange-doped nonaligned and rub-aligned P3HT films using both the Hall bar and rectangular electrode geometries.

Doping Method	Hall Parameters	Rectangular nonaligned	Hall bar nonaligned	Rectangular aligned ( $\parallel, \perp$ )	Hall bar aligned ( $\parallel, \perp$ )
Conventional	Hall carrier density ( $\text{cm}^{-3}$ )	$3.7 \times 10^{20} \pm 1.3 \times 10^{19}$	$4.2 \times 10^{20} \pm 1.9 \times 10^{20}$	$6.2 \times 10^{20} \pm 1.4 \times 10^{20}$	$3.3 \times 10^{20} \pm 8.7 \times 10^{19}, 1.0 \times 10^{21} \pm 1.0 \times 10^{21}$
	Mobility ( $\text{cm}^2/\text{V s}$ )	$0.08 \pm 0.005$	$0.09 \pm 0.06$	$0.08 \pm 0.02, 0.007 \pm 0.002$	$0.2 \pm 0.09, 0.01 \pm 0.008$
Anion-exchange	Hall carrier density ( $\text{cm}^{-3}$ )	$4.7 \times 10^{20} \pm 3.6 \times 10^{19}$	$4.3 \times 10^{20} \pm 5.4 \times 10^{19}$	$9.0 \times 10^{20} \pm 5.8 \times 10^{19}$	$5.5 \times 10^{19} \pm 4.5 \times 10^{19}, 8.7 \times 10^{20} \pm 7.7 \times 10^{20}$
	Mobility ( $\text{cm}^2/\text{V s}$ )	$0.17 \pm 0.01$	$0.16 \pm 0.03$	$0.24 \pm 0.03, 0.022 \pm 0.004$	$7.10 \pm 3.11, 0.03 \pm 0.02$

different carrier density being measured in the parallel and perpendicular directions for the Hall bar geometry. This trend is also consistent with having mixed transport.

As mentioned previously, in earlier work, Brinkmann and co-workers used a four-line geometry [Fig. 1(c)] to measure the anisotropic conductivity of rub-aligned doped conjugated polymer films [7–13]. To calculate the conductivity for the four-line geometry, Brinkmann and coworkers added a geometrical correction factor  $C$  to the standard four-point probe equation to account for the use of lines instead of point-like electrodes, as summarized in Eq. (6) [7,9],

$$\sigma = \frac{\ln(2)}{C\pi} \frac{I}{\Delta V} \frac{1}{t}, \quad (6)$$

where  $\Delta V$  is the measured voltage between the two inner electrodes,  $I$  is the current sourced between the two outer electrodes, and  $t$  is the film's thickness. The geometrical correction factor is obtained by taking the ratio of resistances obtained from four-point and four-line electrode geometries on nonaligned films [7,9]. For our four-line geometry (1.5-mm spacing between 7.5-mm-long electrodes), the correction factor was measured to be approximately 1.4, as described in the Supplemental Material [26]. It is also important to point out that the four-line geometry used by Brinkmann and coworkers, shown in Fig. 1(c), has square contacts at one end. The smaller correction factor we found here compared to that reported by Hamidi-Sakr *et al.* ( $C = 1.8$ ) [9] likely results from our use of different electrode sizes relative to the sample area.

We then used Eq. (8), along with the value of 1.4 for the geometrical correction factor  $C$ , to calculate the conductivity of rub-aligned doped P3HT films using the four-line electrode geometry [Fig. 1(c)]; the results are summarized in Table III. The rub-aligned films for this comparison were made in the same way as those whose properties are

shown in Fig. 3 and Table I, except that the films were sequentially doped using a 1-mg/ml  $\text{F}_4\text{TCNQ}$  solution in acetonitrile (instead of  $n$ -BA) to directly compare with the previous work by Untilova *et al.* [7]. Table III shows that the parallel and perpendicular conductivities obtained using the four-line geometry are around 26% and 40% higher than those obtained using the rectangular geometry, respectively. This overestimation of conductivity using the four-line geometry is likely why Huang *et al.* [19], who used the Hall bar geometry to measure the electrical conductivity of rub-aligned doped conjugated polymer films, were unable to reproduce the high conductivities reported by Vijayakumar *et al.* [14].

To understand why the four-line geometry overestimates the conductivity, we performed a set of additional experiments involving further modification to this electrode geometry. First, we created an electrode geometry with four uniform lines that did not have square contact pads [Fig. 1(d)]. When measured on isotropic doped P3HT samples, the correction factor remained at the same value of 1.4 as for the geometry with the square contact pads (Table S4 in the Supplemental Material [26]). However, we found a notable difference when applying this modified four-line electrode geometry to the aligned doped P3HT samples: the configuration featuring square contacts yielded a higher conductivity in both the parallel and perpendicular directions, as summarized in Table III. This suggests that the use of a single correction factor that is derived from an isotropic sample cannot be rigorously applied to measuring anisotropic conductivity. We believe that this explains why Untilova *et al.* saw an apparent increase in conductivity in the perpendicular direction of their aligned samples relative to isotropic samples [7]: the isotropic correction factor is too low to properly describe the perpendicular carrier transport.

Next, we examined another factor that might explain why the four-line geometry electrodes in Fig. 1(c) lead to

TABLE III. Conductivities of rub-aligned F<sub>4</sub>TCNQ-doped P3HT films in different directions using the rectangular [Fig. 1(b)] and various four-line [Figs. 1(c)–1(e)] electrode geometries.

Electrode geometry	Parallel conductivity (S/cm)	Perpendicular conductivity (S/cm)
Rectangular [Montgomery method; Fig. 1(b), this work]	$2.59 \pm 0.09$	$0.21 \pm 0.01$
Four-line [Hamidi-Sakr <i>et al.</i> [9]; Fig. 1(c)]	$3.51 \pm 0.22$	$0.36 \pm 0.02$
Four-line [without square contacts; Fig. 1(d)]	$2.80 \pm 0.09$	$0.28 \pm 0.03$
Four-line [without square contacts and confined; Fig 1(e)]	$3.27 \pm 0.02$	$0.20 \pm 0.02$

errors in the measured conductivity: the fact that line electrodes do not span the entire size of the doped polymer sample. The issue is that conducting material “outside” the electrodes may provide for additional current paths that are not reflected in the voltage measured on the center electrodes [21]. To test this, we performed experiments removing the doped aligned polymer material outside the electrodes, which we refer to as the four-line “confined” geometry [Fig. 1(e)]. We found that the four-line confined geometry led to an increase in the measured conductivity in the parallel direction and a decrease in conductivity in the perpendicular direction, thus increasing the measured conductivity anisotropy. This is yet another sign that the use of a single correction factor from an isotropic sample cannot account for electrode geometric disparities used on anisotropically conducting samples. It also likely explains why the conductivity anisotropy we measured with the confined Hall bar and Montgomery electrode geometries was higher than that reported by Untilova *et al.* with the “unconfined” four-line geometry [7].

### III. CONCLUSIONS

In summary, the anisotropic conductivity of rub-aligned doped conjugated polymer films can be accurately measured using the rectangular electrode geometry via the modified Montgomery method. In addition to comparing the Hall bar and rectangular electrode geometries, we showed that use of a four-line geometry, particularly one with square contact pads, significantly overestimates the anisotropic conductivity of rub-aligned films, a result stemming from the fact that the correction factor measured on isotropic films does not properly transfer to anisotropically conducting samples. Overall, the rectangular geometry is significantly more straightforward to fabricate than the Hall bar geometry and allows the conductivity in both directions to be measured simultaneously, making it a better alternative to the Hall bar and four-line geometries for anisotropic conductivity measurements of rub-aligned doped conjugated polymers, although the Hall bar geometry is still preferred for Hall effect measurements.

The data that support the findings of this study are available from the corresponding author upon reasonable request.

### ACKNOWLEDGMENTS

This work was supported by the National Science Foundation under Grants No. CHE-2305152 and No. DMR-2105896. This work also made use of the Stanford Synchrotron Radiation Lightsource, SLAC National Accelerator Laboratory, and is supported by the U.S. Department of Energy, Office of Science, Office of Basic Energy Sciences under Contract No. DE-AC02-76SF00515.

The authors declare that there are no conflicts of interest.

- [1] T. M. Swager, 50th anniversary perspective: Conducting/semiconducting conjugated polymers. A personal perspective on the past and the future, *Macromolecules* **50**, 4867 (2017).
- [2] N. Dubey and M. Leclerc, Conducting polymers: Efficient thermoelectric materials, *J. Polym. Sci., Part B: Polym. Phys.* **49**, 467 (2011).
- [3] G.-H. Kim, L. Shao, K. Zhang, and K. P. Pipe, Engineered doping of organic semiconductors for enhanced thermoelectric efficiency, *Nat. Mater.* **12**, 8 (2013).
- [4] R. Noriega, J. Rivnay, K. Vandewal, F. P. V. Koch, N. Stingelin, P. Smith, M. F. Toney, and A. Salleo, A general relationship between disorder, aggregation and charge transport in conjugated polymers, *Nat. Mater.* **12**, 11 (2013).
- [5] G. Zuo, Z. Li, O. Andersson, H. Abdalla, E. Wang, and M. Kemerink, Molecular doping and trap filling in organic semiconductor host-guest systems, *J. Phys. Chem. C* **121**, 7767 (2017).
- [6] H. T. Yi, Y. N. Gartstein, and V. Podzorov, Charge carrier coherence and Hall effect in organic semiconductors, *Sci. Rep.* **6**, 1 (2016).
- [7] V. Untilova, T. Biskup, L. Biniak, V. Vijayakumar, and M. Brinkmann, Control of chain alignment and crystallization helps enhance charge conductivities and thermoelectric power factors in sequentially doped P3HT : F<sub>4</sub>TCNQ films, *Macromolecules* **53**, 2441 (2020).
- [8] Laure Biniak, Stéphanie Pouget, David Djurado, Eric Gonthier, Kim Tremel, Navaphun Kayunkid, Elena Zaborova, Nicolas Crespo-Monteiro, Olivier Boyron, Nicolas Leclerc *et al.*, High-temperature rubbing: A versatile method to align  $\pi$ -conjugated polymers without alignment substrate, *Macromolecules* **47**, 3871 (2014).
- [9] A. Hamidi-Sakr, L. Biniak, J.-L. Bantignies, D. Maurin, L. Herrmann, N. Leclerc, P. Lévêque, V. Vijayakumar, N. Zimmermann, and M. Brinkmann, A versatile method to fabricate highly in-plane aligned conducting polymer films



- with anisotropic charge transport and thermoelectric properties: The key role of alkyl side chain layers on the doping mechanism, *Adv. Funct. Mater.* **27**, 1700173 (2017).
- [10] Viktoriia Untilova, Jonna Hynynen, Anna I. Hofmann, Dorothea Scheunemann, Yadong Zhang, Stephen Barlow, Martijn Kemerink, Seth R. Marder, Laure Biniek, Christian Müller *et al.*, High thermoelectric power factor of poly(3-hexylthiophene) through in-plane alignment and doping with a molybdenum dithiolene complex, *Macromolecules* **53**, 6314 (2020).
- [11] Y. Zhong, V. Untilova, D. Muller, S. Guchait, C. Kiefer, L. Herrmann, N. Zimmermann, M. Brosset, T. Heiser, and M. Brinkmann, Preferential location of dopants in the amorphous phase of oriented regioregular poly(3-hexylthiophene-2,5-diyl) films helps reach charge conductivities of  $3000 \text{ S cm}^{-1}$ , *Adv. Funct. Mater.* **32**, 2202075 (2022).
- [12] V. Untilova, H. Zeng, P. Durand, L. Herrmann, N. Leclerc, and M. Brinkmann, Intercalation and ordering of F<sub>6</sub>TCNNQ and F<sub>4</sub>TCNQ dopants in regioregular poly(3-hexylthiophene) crystals: Impact on anisotropic thermoelectric properties of oriented thin films, *Macromolecules* **54**, 6073 (2021).
- [13] V. Vijayakumar, P. Durand, H. Zeng, V. Untilova, L. Herrmann, P. Algayer, N. Leclerc, and M. Brinkmann, Influence of dopant size and doping method on the structure and thermoelectric properties of PBTTT films doped with F<sub>6</sub>TCNNQ and F<sub>4</sub>TCNQ, *J. Mater. Chem. C* **8**, 16470 (2020).
- [14] V. Vijayakumar, Y. Zhong, V. Untilova, M. Bahri, L. Herrmann, L. Biniek, N. Leclerc, and M. Brinkmann, Bringing conducting polymers to high order: Toward conductivities beyond  $105 \text{ S cm}^{-1}$  and thermoelectric power factors of  $2 \text{ mW m}^{-1} \text{ K}^{-2}$ , *Adv. Energy Mater.* **9**, 1900266 (2019).
- [15] J. Li, M. Xue, N. Xue, H. Li, L. Zhang, Z. Ren, S. Yan, and X. Sun, Highly anisotropic P3HT film fabricated via epitaxy on an oriented polyethylene film and solvent vapor treatment, *Langmuir* **35**, 7841 (2019).
- [16] S. Qu, Q. Yao, L. Wang, Z. Chen, K. Xu, H. Zeng, W. Shi, T. Zhang, C. Uher, and L. Chen, Highly anisotropic P3HT films with enhanced thermoelectric performance via organic small molecule epitaxy, *NPG Asia Mater.* **8**, 7 (2016).
- [17] Y. Xu, X. Wang, J. Zhou, B. Song, Z. Jiang, E. M. Y. Lee, S. Huberman, K. K. Gleason, and G. Chen, Molecular engineered conjugated polymer with high thermal conductivity, *Sci. Adv.* **4**, eaar3031 (2018).
- [18] A. Salleo, Charge transport in polymeric transistors, *Mater. Today* **10**, 38 (2007).
- [19] Yuxuan Huang, Dionisius Hardjo Lukito Tjhe, Ian Jacobs, Xuechen Jiao, Qiao He, Martin Statz, Xinglong Ren, Xinyi Huang, Iain McCulloch, Martin Heeney *et al.*, Design of experiment optimization of aligned polymer thermoelectrics doped by ion-exchange, *Appl. Phys. Lett.* **119**, 111903 (2021).
- [20] C. A. M. dos Santos, A. de Campos, M. S. da Luz, B. D. White, J. J. Neumeier, B. S. de Lima, and C. Y. Shigue, Procedure for measuring electrical resistivity of anisotropic materials: A revision of the Montgomery method, *J. Appl. Phys.* **110**, 083703 (2011).
- [21] I. Miccoli, F. Edler, H. Pfnür, and C. Tegenkamp, The 100th anniversary of the four-point probe technique: The role of probe geometries in isotropic and anisotropic systems, *J. Phys.: Condens. Matter* **27**, 223201 (2015).
- [22] H. C. Montgomery, Method for measuring electrical resistivity of anisotropic materials, *J. Appl. Phys.* **42**, 2971 (1971).
- [23] J. D. Wasscher, Note on four-point resistivity measurements on anisotropic conductors, *Philips Res. Rep.* **301**, 301 (1961).
- [24] L. J. van der Pauw, Determination of resistivity tensor and Hall tensor of anisotropic conductors, *Philips Res. Rep.* **16**, 187 (1961).
- [25] B. F. Logan, S. O. Rice, and R. F. Wick, Series for computing current flow in a rectangular block, *J. Appl. Phys.* **42**, 2975 (1971).
- [26] See Supplemental Material <http://link.aps.org/supplemental/10.1103/PhysRevApplied.21.024006> for thin-film fabrication methods, polarized UV-vis spectroscopy data, grazing-incidence wide-angle x-ray scattering, conductivity and Hall effect measurements, four-line geometry correction factor, profilometry, and temperature-dependent conductivity measurements data, including those from Refs. [27–29].
- [27] J. Lindemuth and S.-I. Mizuta, in *Thin Film Solar Technology III*, edited by L. A. Eldada (SPIE, San Diego, 2011), Vol. 8110, pp. 65–71.
- [28] F. Werner, Hall measurements on low-mobility thin films, *J. Appl. Phys.* **122**, 13 (2017).
- [29] Taylor J. Aubry, Jonathan C. Axtell, Victoria M. Basile, K. J. Winchell, Jeffrey R. Lindemuth, Tyler M. Porter, Ji-Yuan Liu, Anastassia N. Alexandrova, Clifford P. Kubiak, Sarah H. Tolbert *et al.*, Dodecaborane-based dopants designed to shield anion electrostatics lead to increased carrier mobility in a doped conjugated polymer, *Adv. Mater.* **31**, 11 (2019).
- [30] K. J. Winchell, M. G. Voss, B. J. Schwartz, and S. H. Tolbert, Understanding the effects of confinement and crystallinity on HJ-coupling in conjugated polymers via alignment and isolation in an oriented mesoporous silica host, *J. Phys. Chem. C* **125**, 23240 (2021).
- [31] D. T. Scholes, P. Y. Yee, J. R. Lindemuth, H. Kang, J. Onorato, R. Ghosh, C. K. Luscombe, F. C. Spano, S. H. Tolbert, and B. J. Schwartz, The effects of crystallinity on charge transport and the structure of sequentially processed F<sub>4</sub>TCNQ-doped conjugated polymer films, *Adv. Funct. Mater.* **27**, 44 (2017).
- [32] F. C. Spano, Modeling disorder in polymer aggregates: The optical spectroscopy of regioregular poly(3-hexylthiophene) thin films, *J. Chem. Phys.* **122**, 234701 (2005).
- [33] D. T. Scholes, S. A. Hawks, P. Y. Yee, H. Wu, J. R. Lindemuth, S. H. Tolbert, and B. J. Schwartz, Overcoming film quality issues for conjugated polymers doped with F<sub>4</sub>TCNQ by solution sequential processing: Hall effect, structural, and optical measurements, *J. Phys. Chem. Lett.* **6**, 4786 (2015).
- [34] S. A. Hawks, J. C. Aguirre, L. T. Schelhas, R. J. Thompson, R. C. Huber, A. S. Ferreira, G. Zhang, A. A. Herzing, S. H. Tolbert, and B. J. Schwartz, Comparing matched polymer:fullerene solar cells made by solution-sequential

- processing and traditional blend casting: Nanoscale structure and device performance, *J. Phys. Chem. C* **118**, 17413 (2014).
- [35] J. C. Aguirre, S. A. Hawks, A. S. Ferreira, P. Yee, S. Subramanian, S. A. Jenekhe, S. H. Tolbert, and B. J. Schwartz, Sequential processing for organic photovoltaics: Design rules for morphology control by tailored semi-orthogonal solvent blends, *Adv. Energy Mater.* **5**, 11 (2015).
- [36] Y. Yamashita, J. Tsurumi, M. Ohno, R. Fujimoto, S. Kumagai, T. Kurosawa, T. Okamoto, J. Takeya, and S. Watanabe, Efficient molecular doping of polymeric semiconductors driven by anion exchange, *Nature* **572**, 634 (2019).
- [37] Y. Wu, Q. M. Duong, A. F. Simafranca, C. Z. Salamat, B. J. Schwartz, and S. H. Tolbert, *ACS Mater. Lett.* **4**, 489 (2024).
- [38] B. J. Boehm, H. T. L. Nguyen, and D. M. Huang, The interplay of interfaces, supramolecular assembly, and electronics in organic semiconductors, *J. Phys.: Condens. Matter* **31**, 423001 (2019).
- [39] Y. Hosokawa, M. Misaki, S. Yamamoto, M. Torii, K. Ishida, and Y. Ueda, Molecular orientation and anisotropic carrier mobility in poorly soluble polythiophene thin films, *Appl. Phys. Lett.* **100**, 203305 (2012).
- [40] H. S. Lee, J. H. Cho, K. Cho, and Y. D. Park, Alkyl side chain length modulates the electronic structure and electrical characteristics of poly(3-alkylthiophene) thin films, *J. Phys. Chem. C* **117**, 11764 (2013).
- [41] R. Joseph Kline, M. D. McGehee, and M. F. Toney, Highly oriented crystals at the buried interface in polythiophene thin-film transistors, *Nat. Mater.* **5**, 3 (2006).
- [42] J. Zhao, Y. Li, G. Yang, K. Jiang, H. Lin, H. Ade, W. Ma, and H. Yan, Efficient organic solar cells processed from hydrocarbon solvents, *Nat. Energy* **1**, 2 (2016).
- [43] H. Lee, D. Lee, D. H. Sin, S. W. Kim, M. S. Jeong, and K. Cho, Effect of donor–acceptor molecular orientation on charge photogeneration in organic solar cells, *NPG Asia Mater.* **10**, 6 (2018).
- [44] T. J. Aubry, A. S. Ferreira, P. Y. Yee, J. C. Aguirre, S. A. Hawks, M. T. Fontana, B. J. Schwartz, and S. H. Tolbert, Processing methods for obtaining a face-on crystalline domain orientation in conjugated polymer-based photovoltaics, *J. Phys. Chem. C* **122**, 15078 (2018).
- [45] C. Piliago, T. W. Holcombe, J. D. Douglas, C. H. Woo, P. M. Beaujuge, and J. M. J. Fréchet, Synthetic control of structural order in *N*-alkylthieno[3,4-*c*]pyrrole-4,6-dione-based polymers for efficient solar cells, *J. Am. Chem. Soc.* **132**, 7595 (2010).
- [46] P. Y. Yee, D. T. Scholes, B. J. Schwartz, and S. H. Tolbert, Dopant-induced ordering of amorphous regions in regiorandom P3HT, *J. Phys. Chem. Lett.* **10**, 17 (2019).
- [47] O. Bierwagen, R. Pomraenke, S. Eilers, and W. T. Masselink, Mobility and carrier density in materials with anisotropic conductivity revealed by van der Pauw measurements, *Phys. Rev. B* **70**, 165307 (2004).
- [48] Y. Chen, H. T. Yi, and V. Podzorov, High-resolution ac measurements of the Hall effect in organic field-effect transistors, *Phys. Rev. Appl.* **5**, 034008 (2016).
- [49] Zhiming Liang, Hyun Ho Choi, Xuyi Luo, Tuo Liu, Ashkan Abtahi, Uma Shantini Ramasamy, J. Andrew Hitron, Kyle N. Baustert, Jacob L. Hempel, Alex M. Boehm *et al.*, n-type charge transport in heavily p-doped polymers, *Nat. Mater.* **20**, 518 (2021).
- [50] S. A. Gregory, R. Hanus, A. Atassi, J. M. Rinehart, J. P. Wooding, A. K. Menon, M. D. Losego, G. J. Snyder, and S. K. Yee, Quantifying charge carrier localization in chemically doped semiconducting polymers, *Nat. Mater.* **20**, 1414 (2021).